Asian Journal of Atmospheric Environment
Vol. 11, No. 2, pp. 96-106, June 2017
doi: https://doi.org/10.5572/ajae.2017.11.2.096
ISSN (Online) 2287-1160, ISSN (Print) 1976-6912

Chemical and Absorption Characteristics of Water-soluble Organic Carbon and Humic-like Substances in Size-segregated Particles from Biomass Burning Emissions

Jaemyeong Yu, Geun-Hye Yu, Seungshik Park* and Min-Suk Bae[1)]

Department of Environment and Energy Engineering, Chonnam National University, 77 Yongbong-ro, Buk-ku, Gwangju 61186, Republic of Korea
[1)]Department of Environmental Engineering, Mokpo National University, Jeolanam-do, Mokpo, Republic of Korea

*Corresponding author. Tel: +82-62-530-1863, E-mail: park8162@chonnam.ac.kr

ABSTRACT

In this study, measurements of size-segregated particulate matter (PM) emitted from the combustion of rice straw, pine needles, and sesame stem were conducted in a laboratory chamber. The collected samples were used to analyze amounts of organic and elemental carbon (OC and EC), water-soluble organic carbon (WSOC), humic-like substances (HULIS), and ionic species. The light absorption properties of size-resolved water extracts were measured using ultraviolet-visible spectroscopy. A solid-phase extraction method was first used to separate the size-resolved HULIS fraction, which was then quantified by a total organic carbon analyzer. The results show that regardless of particle cut sizes, the contributions of size-resolved HULIS (=1.94×HULIS-C) to PM size fractions ($PM_{0.32}$, $PM_{0.55}$, $PM_{1.0}$, and $PM_{1.8}$) were similar, accounting for 25.2-27.6, 15.2-22.4 and 28.2-28.7% for rice straw, pine needle, and sesame stem smoke samples, respectively. The $PM_{1.8}$ fraction revealed WSOC/OC and HULIS-C/WSOC ratios of 0.51 and 0.60, 0.44 and 0.40, and 0.50 and 0.60 for the rice straw, pine needle, and sesame stem burning emissions, respectively. Strong absorption with decreasing wavelength was found by the water extracts from size-resolved biomass burning aerosols. The absorption Ångström exponent values of the size-resolved water extracts fitted between 300 and 400 nm wavelengths for particle sizes of 0.32-1.0 μm were 6.6-7.7 for the rice straw burning samples, and 7.5-8.0 for the sesame stem burning samples. The average mass absorption efficiencies of size-resolved WSOC and HULIS-C at 365 nm were 1.09 (range: 0.89-1.61) and 1.82 (range: 1.33-2.06) $m^2/g \cdot C$ for rice straw smoke aerosols, and 1.13 (range: 0.85-1.52) and 1.83 (range: 1.44-2.05) $m^2/g \cdot C$ for sesame stem smoke aerosols, respectively. The light absorption of size-resolved water extracts measured at 365 nm showed strong correlations with WSOC and HULIS-C concentrations (R^2=0.89-0.93), indicating significant contribution of HULIS component from biomass burning emissions to the light absorption of ambient aerosols.

Key words: Size-segregated biomass burning aerosols, WSOC, HULIS, Absorption Ångström exponent, Mass absorption efficiency

1. INTRODUCTION

Biomass burning (BB) plumes, including aerosols from forest fires and agricultural residuals burning, have drawn great attention, due to their impact on air quality, visibility, human health, and global radiative forcing (Park and Son, 2017; Laskin *et al*., 2015 and references therein; Andreae and Gelencsér, 2006). BB emits huge amounts of particulate organic carbon (OC) to the atmosphere. In general, OC aerosols have been identified as a scatter of solar radiation, but some components of OC also show significant light absorption in the near UV (300-400 nm) and visible wavelength regions (Laskin *et al*., 2015; Andreae and Gelencsér, 2006). This type of OC, termed brown carbon, mainly originates from BB emissions or secondary formation in the air (Park and Yu, 2016; Liu *et al*., 2013; Chen and Bond, 2010; Hecobian *et al*., 2010; Andreae and Gelencsér, 2006), and is an important contributor of aerosol light absorption, resulting in warming effects.

Water-soluble OC (WSOC), which constitutes a significant amount of atmospheric OC, is formed as by-products of atmospheric oxidation reactions of organic compounds, as well as the primary BB emissions, with a small contribution from the fossil fuel combustion (Park and Yu, 2016; Yu *et al*., 2014; Weber *et al*.,

2007). Furthermore, the WSOC is often considered an indicator of secondary organic aerosol formation (Kuang *et al*., 2015; Yu *et al*., 2014; Weber *et al*., 2007). Based on the carbon chain length and number of functional group per molecule, the WSOC can broadly be classified into hydrophilic and hydrophobic fractions (Park *et al*., 2015, 2013a, 2012; Park and Kim, 2014; Duarte and Duarte, 2005). Humic-like Substances (HULIS) may influence the indirect climate forcing of the atmospheric aerosols by modifying the microphysical properties of cloud droplets (Dinar *et al*., 2006; Fuzzi *et al*., 2006) and also contributes to positive climate radiative forcing, by absorbing the solar radiation in the near ultraviolet and visible ranges (Laskin *et al*., 2015; Kirillova *et al*., 2014; Chen and Bond, 2010; Hoffer *et al*., 2006). Previous studies have indicated that atmospheric HULIS are emitted from BB (Fan *et al*., 2016a; Park and Son, 2016; Park and Yu, 2016; Lin *et al*., 2010a; Salma *et al*., 2010), or are formed by secondary processes (Park and Son, 2016; Kuang *et al*., 2015; Son *et al*., 2015; Lin *et al*., 2010a; Altieri *et al*., 2009). It has been reported that the HULIS in the air contribute significantly to the WSOC with a greater contribution in BB-influenced ambient aerosol samples (Fan *et al*., 2016b; Son *et al*., 2015; Lin *et al*., 2010a, b; Mayol-Bracero *et al*., 2002), and are higher in winter than in summer (Fan *et al*., 2016b; Son *et al*., 2015; Baduel *et al*., 2010; Krivácsy *et al*., 2008). In fresh BB emissions, the HULIS-C fraction (based on a carbon mass) in $PM_{2.5}$ contributed 15-33% (Lin *et al*., 2010a; Mayol-Bracero *et al*., 2002) and 63-76% of WSOC (Salma *et al*., 2010). However, our previous study (Park and Yu, 2016), which was conducted in a laboratory chamber environment, indicated that the HULIS-C constituted 36-63% of WSOC in $PM_{2.5}$, which varied with the biomass materials burned. The significant difference in contribution of HULIS to WSOC from BB emissions is likely ascribed to the biomass materials burned, burning condition (smoldering vs. flaming), burning temperature, and methods for isolation and quantification of HULIS (Park and Yu, 2016; Zheng *et al*., 2013; Chen and Bond, 2010; Lin *et al*., 2010a, b; Lukács *et al*., 2007; Hoffer *et al*., 2006; Duarte *et al*., 2005).

Size-resolved chemical composition of both particles from emission sources and ambient air particles is essential to understand their origin and formation, and the extent of aging of the atmospheric particles (Seinfeld and Pandis, 2006). However, to the best of our knowledge, studies on the size distribution of HULIS are extremely limited. For example, Lin *et al*. (2010a) has shown that the size distribution of ambient HULIS at a rural site in China, had a dominant droplet mode that peaked at 0.63-0.87 μm, which was attributed to the growth of fresh condensation mode BB particles through in-cloud processing and to the secondary formation processes. Further, a recent study that was conducted during winter at an urban site in Korea (Park and Son, 2016), indicated that the HULIS exhibited a unimodal size distribution that peaked in the size range of 0.55-1.0 μm during the non-Asian dust period, and a bimodal distribution that peaked in the size ranges of at 0.32-0.55 μm and 1.8-3.1 μm during the Asian dust period.

Studies associated with the light absorption of bulk aerosol particles in biomass burning emissions and ambient air have extensively been conducted in East Asia (Cheng *et al*., 2016; Kim *et al*., 2016; Li *et al*., 2016; Park and Yu, 2016; Du *et al*., 2014; Kirillova *et al*., 2014). For example, our group most recently investigated the light absorption properties of water-soluble extracts of fine particulate matter emitted from BB in a laboratory chamber environment (Park and Yu, 2016). However, information on the size distribution of HULIS and light absorption properties of size-resolved WSOC from BB emissions has not yet been reported. Understanding of the chemical and light absorption characteristics of size-segregated biomass burning aerosols is very important for improving air quality, and evaluating the warming effect on the Earth. Knowledge of the light absorption by brown carbon aerosols from BB emissions is particularly important. Therefore, this study was initiated to investigate the chemical and optical characteristics of water-soluble HULIS in size-resolved particles emitted from the combustion of three biomass materials (rice straw, pine needle, and sesame stem) in a laboratory test chamber. Results from this study can help improve our understanding of the sources and formation processes, and light absorption properties of size-segregated HULIS in ambient environments.

2. METERIALS AND METHODS

2.1 Collection of Size-segregated Samples from Biomass Burning Emissions

A Micro-Orifice Uniform Deposit Impactor (MOUDI, MSP 110; MSP Corp., MN) was utilized to collect size-segregated particulate matter emitted from the combustion of biomass materials in a laboratory hood chamber. Three types of biomass materials (rice straw, pine needles, and sesame stems) were used in this study. The rice straw and sesame stem materials were collected at rural farmlands, and the pine needles were collected from a small park near a two-lane road. The emission rates of smoke particles from BB emissions were not measured.

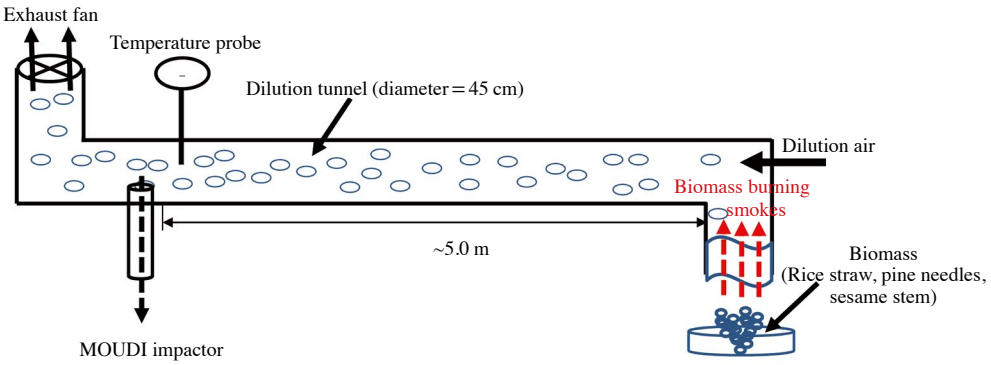

Fig. 1. A schematic of the sampling apparatus from biomass burning emissions.

Fig. 1 shows a schematic of the sampling system, which includes a combustion pan, dilution tunnel, clean background air injection port, exhaust fan hood, and MOUDI. Details of the sampling system are provided in our previous publication (Park and Yu, 2016). The sampling flow rate of the MOUDI was 30 L/min. The 10-stage MOUDI has cut-off diameters of 0.055, 0.095, 0.17, 0.32, 0.55, 1.00, 1.8, 3.1, 6.2, 9.9, and 18.0 μm. MOUDI samples from the combustion of biomass materials were collected onto prebaked and pre-weighed 47-mm quartz-fiber filters (Pall Gelman, Ann Arbor, MI). Combustion tests were conducted three times for each of the biomass materials, and three sets of MOUDI samples were collected for each biomass material. Size-segregated measurements of PM smoke samples from BB emissions were made without the carbon denuder that is typically used to minimize the over-determination of organic aerosol concentrations. Measurements of MOUDI samples were performed for approximately 5 minutes at a mixed condition of smoldering and flaming burning. The mass, organic carbon and elemental carbon (OC and EC), total WSOC, HULIS, and ionic species concentrations were determined from the size-segregated PM samples. Blank values of filters were also analyzed, and used to correct the measured concentrations of BB samples in each impactor stage. For OC and EC measurements, only size-segregated samples with particle diameters of 0.055-3.1 μm were quantified.

2.2 Chemical Analysis of Size-segregated PM Samples from BB Emissions

Mass concentrations of size-resolved PM samples were calculated by dividing the difference of the weight before and after collection of the samples into a sampling volume of air. The filter substrates were weighed using a microbalance of 1-μg sensitivity (Sartorius CP2P-F). The filters prior to weighing were conditioned for approximately 24 hr in a desiccator (relative humidity of ~40% and temperature of ~20°C).

The analytical methods for OC, EC, WSOC, water-soluble HULIS, and ionic species from size-resolved PM samples from BB emissions were provided in detail in our previous studies (Park and Yu, 2016 and references therein; Park *et al*., 2015). Briefly, a spot area ranging from 0.186 to 1.00 cm^2, which is varied with the impactor stage (particle mass loaded on a filter), was punched from each filter, and used to determine the amounts of size-resolved OC and EC using the NIOSH thermal-optical transmittance (TOT) standard method. The very small punch area (0.186 cm^2) was due to the high amount of OC in the BB samples. The remaining filters were extracted with 60 mL of distilled deionized water in an ultrasonic bath at room temperature for 60 minutes. The water extracts were filtered with a 0.45 μm membrane filter (Millipore, USA). An ion chromatography (IC) system (Metrohm 861) and a total organic carbon (TOC) analyzer (Sievers 5310C, USA) were used to analyze ionic species (Na^+, NH_4^+, K^+, Ca^{2+}, Mg^{2+}, Cl^-, NO_3^-, SO_4^{2-}, and oxalate) and total WSOC, respectively. The rest of the water extract was used for group separation of HULIS using a hydrophilic-lipophilic balanced (HLB) solid-phase extraction (SPE) method (Park and Son, 2016; Park and Yu, 2016; Lin *et al*., 2010a). HULIS was isolated from water extract using a pretreated SPE cartridge (Oasis HLB, 30 μm, 60 mg/cartridge, Waters, USA). The quantification of the isolated HULIS was then performed using a TOC analyzer.

2.3 Light Absorption by WSOC

Light absorption spectra of the water extracts of size-resolved particles from combustion emissions of three types of biomass materials were investigated by UV-vis spectrophotometry (OPTIZEN POP, Mecasys Co., Ltd., Korea) in wavelength ranges of 300-400 nm at 10 nm intervals. Light absorption at wavelength of 365 nm was also measured. Light absorption values of

blank quart-fiber filters were corrected to obtain the actual light absorption spectra of size-resolved water extracts. The Absorption Ångström Exponent (AAE) of size-resolved water extracts from BB emissions was determined by the following relationship (Laskin *et al*., 2015):

$$\mathrm{AAE} = \frac{-\ln(A(\lambda_1)/A(\lambda_2))}{\ln(\lambda_1/\lambda_2)} \quad (1)$$

Where, $A(\lambda_1)$ and $A(\lambda_2)$ are the measured absorbance at wavelengths of 300 and 400 nm, respectively. The mass absorption efficiency (MAE) of size-resolved water-extracts at 365 nm (MAE_{365}) was calculated by dividing the light absorption of the water extracts into WSOC and HULIS-C concentrations.

$$\mathrm{MAE}_{365}\left(\frac{\mathrm{m}^2}{\mathrm{g}}\right) = \frac{A_{365}}{\mathrm{WSOC\,(or\ HULIS\text{-}C)} \times \mathrm{L}} \times \ln(10) \quad (2)$$

where, A_{365} is the absorbance measured at 365 nm, WSOC and HULIS-C are the concentrations of WSOC and HULIS-C in solution (μg/mL), and L is the absorbing path length (i.e., 1 cm for the currently used quartz cuvettes).

3. RESULTS AND DISCUSSTION

3.1 Mass Balance Closure of Size-resolved PM Samples from BB Emissions

The chemical mass balance closure of size-resolved PM in the cut size ranges of 0.055-3.1 μm from BB emissions was evaluated by comparing the measured and reconstructed size-resolved PM mass concentrations. The following equation was applied to estimate the reconstructed size-resolved PM mass concentration: Reconstructed PM ($\mu g/m^3$) = EC + OM (= WIOM + WSOM) + SIC (= $Na^+ + NH_4^+ + K^+ + Ca^{2+} + Mg^{2+} + Cl^- + NO_3^- + SO_4^{2-}$), where OM, WIOM, WSOM, and SIC represent the organic mass, water-insoluble organic mass, water-soluble organic mass, and sum of ionic components, respectively. Known as the byproducts of incomplete combustion of fossil fuels and biomass materials (Park and Cho, 2011 and references therein), the WIOM was estimated as 1.2 times the WIOC (= OC − WSOC) (Rajput and Sarin, 2014; Turpin and Lim, 2001). Also a multiplying factor of 1.94 was applied to estimate the contribution of WSOM from WSOC (Lin *et al*., 2010a; Kiss *et al*., 2002). Since the amounts of elemental species in the size-resolved PM were not quantified, the contributions of size-resolved elemental species concentrations were not included in the chemical mass balance closure. Fig. 2 shows the regression relationship between the predicted and measured $PM_{0.055\text{-}3.1}$ concentrations for all BB samples, providing a slope and an intercept of 0.87 and 0.08, respectively, with an R^2 of 0.97.

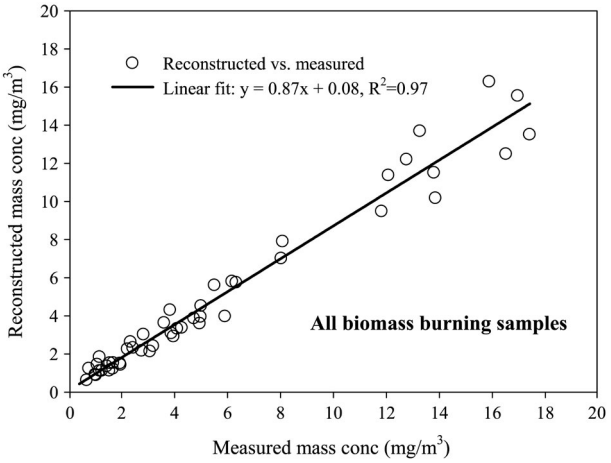

Fig. 2. Comparison of measured and reconstructed size-resolved PM concentrations for all biomass burning emissions.

3.2 Size-resolved Contributions of Chemical Species to PM Fractions for Biomass Type

Fig. 3 shows the size-resolved concentrations of chemical components in smoke samples from BB emissions. In addition, Table 1 shows the contributions of chemical components concentrations to PM size fractions ($PM_{0.32}$, $PM_{0.55}$, $PM_{1.0}$, $PM_{1.8}$) for the smoke emissions of the three biomass materials. Table 1 compares the contribution data of chemical species in $PM_{2.5}$ bulk samples from the burning emissions of the three biomass materials, which were given in our previous publication (Park and Yu, 2016). The table shows that the size-resolved contributions of EC, WIOM, WSOM, HULIS (= 1.94 × HULIS-C), and SIC concentrations to PM size fractions did not show any large difference in particle size for each biomass type. The size-resolved contributions of EC to PM fractions were observed to be higher in pine needle smoke samples than in rice straw and sesame stem smoke samples, but the size-resolved contributions of other chemical species (WIOM, WSOM, HULIS, and SIC) were higher in rice straw and sesame stem smoke samples than in pine needle smoke emissions. For $PM_{1.8}$ fraction, the average contributions of EC, WIOM, WSOM, HULIS, and SIC concentrations to the $PM_{1.8}$ were 2.6, 23.9, 50.7, 27.6 and 8.8% for the rice straw burning emissions, and 7.6, 28.8, 45.2, 27.5

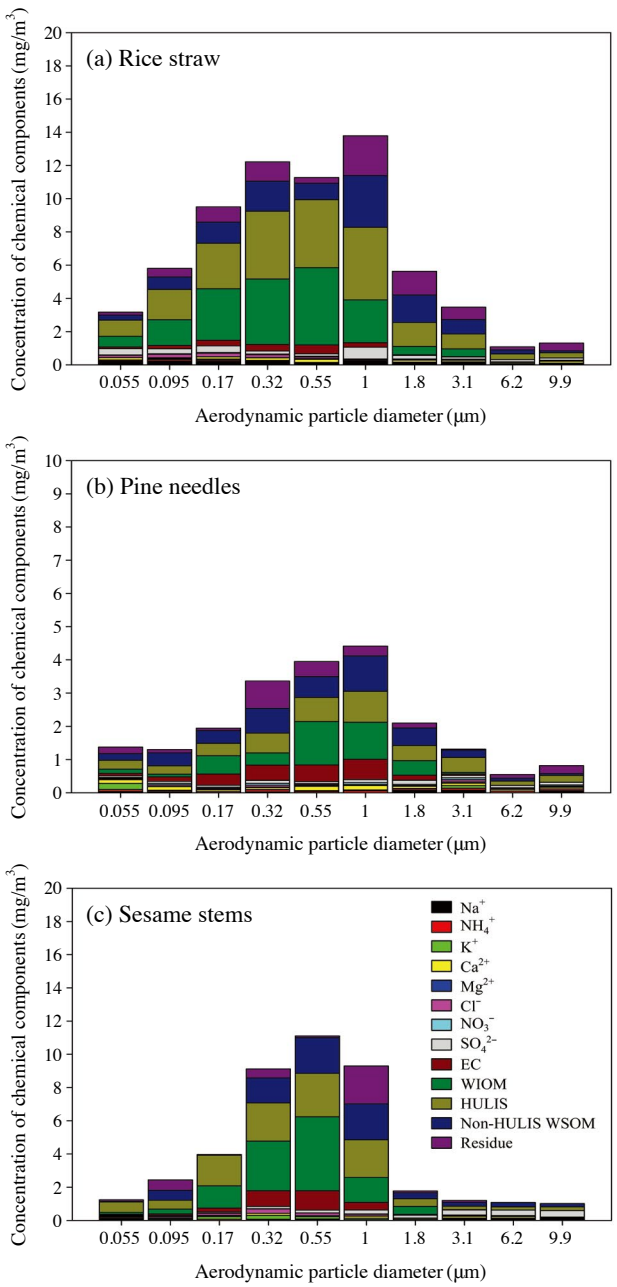

Fig. 3. Size-resolved chemical composition for each biomass type.

and 9.2% for the sesame stem burning emissions, while their contributions in the pine needle burning aerosol samples were 12.6, 22.3, 42.2, 20.2, and 14.3%. The compositional fraction of chemical species in smoke samples from the burning emissions of the three biomass materials were comparable to those from our previous study (Park and Yu, 2016), in which $PM_{2.5}$ smoke samples from burning emissions of the biomass materials (rice straw, pine needle, and sesame stem) in a laboratory combustion chamber were collected and analyzed to determine the concentrations of $PM_{2.5}$, EC, OC, WSOC, HULIS-C, and ionic species. However, lower contributions of WIOM for $PM_{1.8}$ smoke samples from rice straw (23.9%) and pine needle (22.3%) burning emissions were found in this study. Park and Yu (2016) found that the WIOM contributed 39.9, 35.7, and 23.5% to $PM_{2.5}$ smoke samples from rice straw, pine needle, and sesame stem burning emissions, respectively. The OC/EC, WSOC/OC, and HULIS-C/WSOC ratios in $PM_{1.8}$ were 14.4, 0.51, and 0.60 for rice straw burning samples; 3.6, 0.44, and 0.40 for pine needle burning samples; and 6.2, 0.50, and 0.60 for sesame stems burning samples, respectively. The relationships between WSOC and OC, and between HULIS-C and WSOC for all biomass burning smoke samples showed WSOC/OC of 0.51 ($R^2=0.91$) and HULIS-C/WSOC of 0.51 ($R^2=0.94$). These compositional ratios of organic aerosols from BB smoke samples were comparable to those from our previous study (Park and Yu, 2016). The difference in chemical composition in smoke samples from BB emissions could be attributed to the difference in chemical composition of the biomass materials gathered (pine needles at an urban roadway site vs. rice straw and sesame stems at rural fields), and combustion conditions (e.g., burning temperature, burning rate, flaming/smoldering, and amount of materials burned) during combustion of the biomass materials.

3.3 Size Distributions of Carbonaceous Species, K^+, and Cl^- for Biomass Type

Fig. 4 shows the size distributions of OC, EC, WSOC, HULIS-C, K^+, and Cl^- for three biomass types. The figure shows that regardless of biomass type, their size distributions have similar shapes, indicating unimodal size distributions. The dominant modes for EC, OC, WSOC, HULIS-C, K^+, and Cl^- were in the size range of 0.32-1.00 μm for all biomass burning emissions. However, their peaks vary slightly with biomass type. The OC, EC, WSOC, and HULIS-C exhibited unimodal size distributions that peaked between 0.32 and 1.00 μm for the rice straw smoke emissions, and at 0.55 μm for the sesame stem smoke samples, while their size distributions for pine needles smoke emissions peaked at 1.00 μm. The difference in modal diameters of carbonaceous species among the smoke samples from the burning of the three biomass materials was likely due to the difference in burning conditions (temperature, smoldering/flaming, burning rate) and amounts of biomass materials burned, which varied with biomass type during MOUDI measure-

Table 1. Average contribution of chemical species concentration to PM size fractions in burning samples of the three biomass materials.

PM fraction		Unit	Biomass smoke samples		
			Rice straw	Pine needles	Sesame stem
$PM_{0.32}$[1)]	EC	%	2.9	13.4	7.7
	WIOM[2)]		26.5	15.2	28.2
	WSOM[3)]		47.5	43.2	44.5
	HULIS[4)]		27.6	20.1	31.6
	SIC[5)]		11.2	19.5	11.9
$PM_{0.55}$[1)]	EC	%	3.1	13.2	8.8
	WIOM		27.9	21.4	28.2
	WSOM		49.4	40.1	44.5
	HULIS		27.6	19.5	31.6
	SIC		9.2	15.7	11.9
$PM_{1.0}$[1)]	EC	%	2.8	13.4	7.8
	WIOM		25.2	22.4	28.7
	WSOM		50.8	41.6	44.8
	HULIS		27.7	20.0	27.4
	SIC		8.6	13.8	8.8
$PM_{1.8}$[1)]	EC	%	2.6	12.6	7.6
	WIOM		23.9	22.3	28.8
	WSOM		50.7	42.2	45.2
	HULIS		27.6	20.2	27.5
	SIC		8.8	14.3	9.2
	OC/EC	−	14.4	3.6	6.2
	WSOC/OC	−	0.51	0.44	0.50
	HULIS-C/WSOC	−	0.60	0.40	0.60
$PM_{2.5}$[6)]	EC	%	3.5	7.4	4.5
	WIOM		39.9	35.7	23.5
	WSOM		47.5	41.8	49.7
	HULIS		29.5	15.3	25.8
	SIC		12.6	10.2	16.9
	OC/EC	−	16.8	7.0	10.2
	WSOC/OC	−	0.43	0.42	0.57
	HULIS-C/WSOC	−	0.63	0.36	0.51

[1)]PM_{xx} size fraction indicates a size range between 0.055 and xx μm. [2)]WIOM: Water-insoluble organic mass (= 1.2 × WIOC), [3)]WSOM: Water-soluble organic mass (= 1.94 × WSOC), [4)]HULIS: Humic-like substances (= 1.94 × HULIS-C), [5)]SIC: Sum of ionic components ($= Na^+ + NH_4^+ + K^+ + Ca^{2+} + Mg^{2+} + Cl^- + NO_3^- + SO_4^{2-}$), and [6)]Park and Yu (2016).

ments of BB smoke samples. The size distributions of carbonaceous aerosols from BB smoke samples in this study were similar to those from laboratory-generated BB emissions (Park *et al*., 2013b) and from fresh smoke samples from boreal wild fires in Europe (Saarnio *et al*., 2010). Park *et al*. (2013b) found that WSOC and water-soluble ionic species from burning emissions of agricultural crop residues and forest trees showed unimodal size distributions that peaked at 0.32 or 0.55 μm in particle diameter. Size distribution profiles of carbonaceous species, K^+, and Cl^- from BB smokes could provide insights to better understand both the influence of BB plumes on the atmospheric aerosols, and the atmospheric processes of BB affected ambient samples.

3.4 Light Absorption Characteristics of Size-resolved Water Extracts for Biomass Type

As discussed in many previous studies, organic aerosols could absorb solar radiation in the UV (300-400 nm) and visible ranges, as well as light scattering (Laskin *et al*., 2015 and reference herein; Andreae and Gelencsér, 2006). Unfortunately in this study, the light absorption spectra of water-extracts (WSOC) of size-resolved smoke samples from pine needle burning emissions were not measured, due to the contamination of some smoke samples. Fig. 5 shows the light absorption spectra of WSOC over wavelength for three particle sizes (0.32, 0.55, and 1.0 μm) in the rice straw and sesame stem smoke samples. As Fig. 4

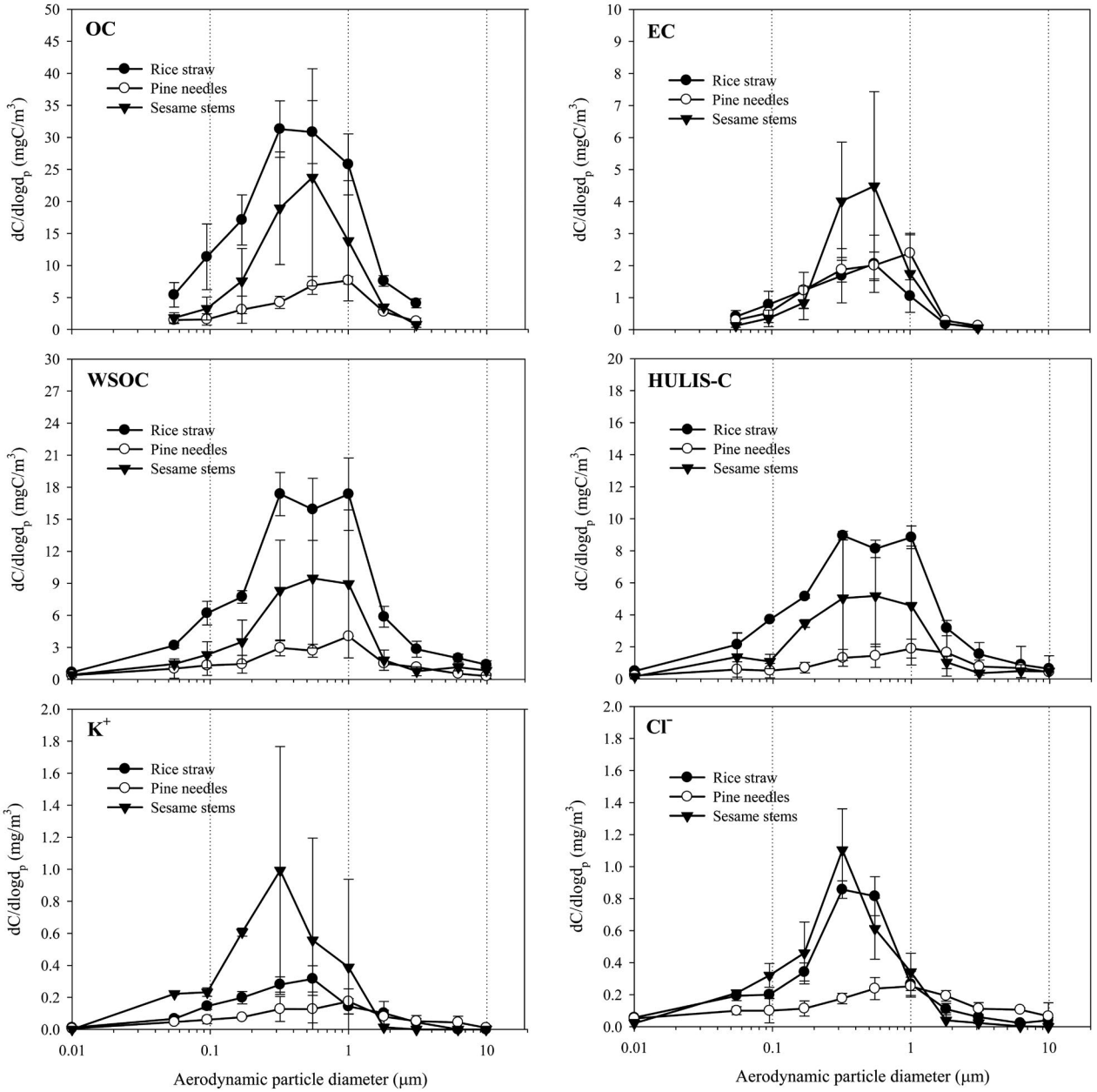

Fig. 4. Mass size distributions of OC, EC, WSOC, HULIS-C, K^+, and Cl^- in aerosol particles from three BB emissions.

shows, the abundances of carbonaceous species in particulate matter from BB emissions are mostly distributed in the particle size range of 0.32-1.0 μm. So, Fig. 5 shows the light absorption spectra of WSOC for only three particle sizes. The figure shows that the light absorption due to WSOC increased sharply towards the shorter wavelengths, which clearly represents the light absorption spectra of brown carbon aerosol. The wavelength-dependent light absorption spectra by WSOC showed less difference among the particle sizes. The AAE of WSOC, which was determined by Eq. (1) described in Section 2.3, for particle size bins of 0.32, 0.55, and 1.0 μm, was 6.6, 7.7 and 7.5 for rice straw burning smoke samples, and 7.5, 8.0 and 7.7 for sesame stem burning smoke samples, respectively. These size-resolved AAE values for BB smoke samples are similar to the AAE values (7~8) of WSOC in $PM_{2.5}$ samples from rice straw, pine needle, and sesame stem burning emissions (Park and Yu, 2016), those of HULIS from the Amazon biomass burning aerosols

(AAE ~7.1) (Hoffer *et al*., 2006), and the results from ambient $PM_{2.5}$ measurements. The AAE values for water extracts in ambient $PM_{2.5}$ samples were in the range of approximately 6.0-9.0 (Cheng *et al*., 2016; Kim *et al*., 2016; Kirillova *et al*., 2014; Zhang *et al*., 2013; Hecobian *et al*., 2010). Not shown in Fig. 5, the AAE values for particle sizes of 0.055, 0.095, 0.17, 1.8, and 3.1 μm were 5.3, 5.1, 7.4, 6.8, and 5.6 for rice straw burning samples, and 4.3, 5.1, 6.6, 6.2, and 4.8 for sesame stem burning samples, respectively. Measurements of size-resolved AAE values from BB smoke samples in this study suggest the dominance of light absorption by condensation and droplet mode WSOC particles (0.32-1.0 μm).

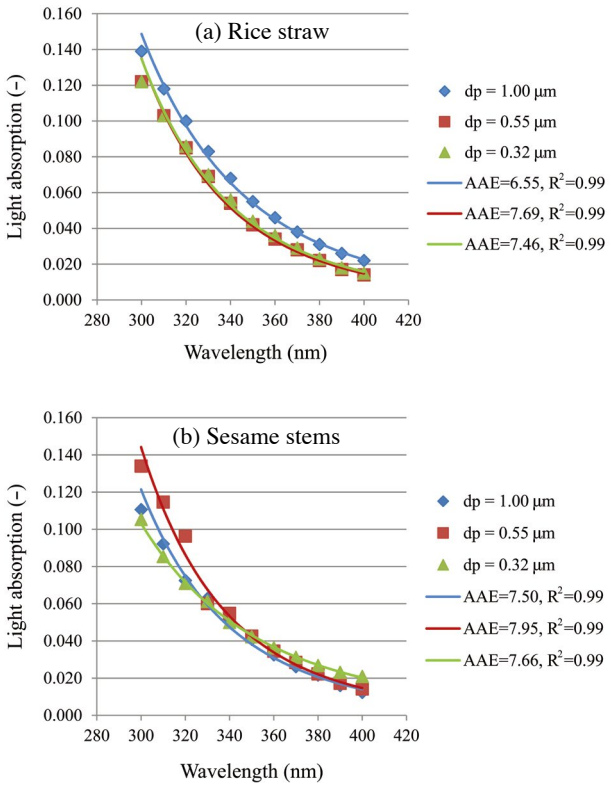

Fig. 5. Size-resolved wavelength dependent light absorption for rice straw and sesame stems burning smoke samples.

Fig. 6 shows correlations of the light absorptions of size-resolved water extracts at 365 nm with WSOC and HULIS-C concentrations (μgC/mL) for rice straw and sesame stem smoke samples. The light absorption of water extracts at 365 nm strongly correlated with the total WSOC and HULIS-C concentrations with R^2 of 0.90 and 0.93, respectively, for rice straw smoke samples, and with R^2 of 0.89 and 0.93, respectively, for sesame stem smoke samples. These results indicate that the water soluble OC and HULIS from BB emissions can strongly absorb light in the near UV wavelength range.

Fig. 7 shows the size-resolved mass absorption efficiencies at 365 nm (MAE_{365}) based on WSOC and HULIS-C concentrations. The figure shows that the size-resolved MAE_{365} values were higher in HULIS-C base than in WSOC base for both BB emissions. Little difference in MAE_{365} between the two BB smoke types was found. For rice straw smoke samples, WSOC- and HULIS-C-based MAE_{365} in the particle size ranges of 0.055-3.1 μm were 0.89-1.61 (average of 1.09) and 1.33-2.06 $m^2/g \cdot C$ (average of 1.82), respectively. Respective MAE_{365} values for sesame stem smoke samples were 0.85-1.52 (average of 1.13) and 1.44-2.05 $m^2/g \cdot C$ (average of 1.83). These WSOC MAE_{365} values were comparable to those (0.86-1.38

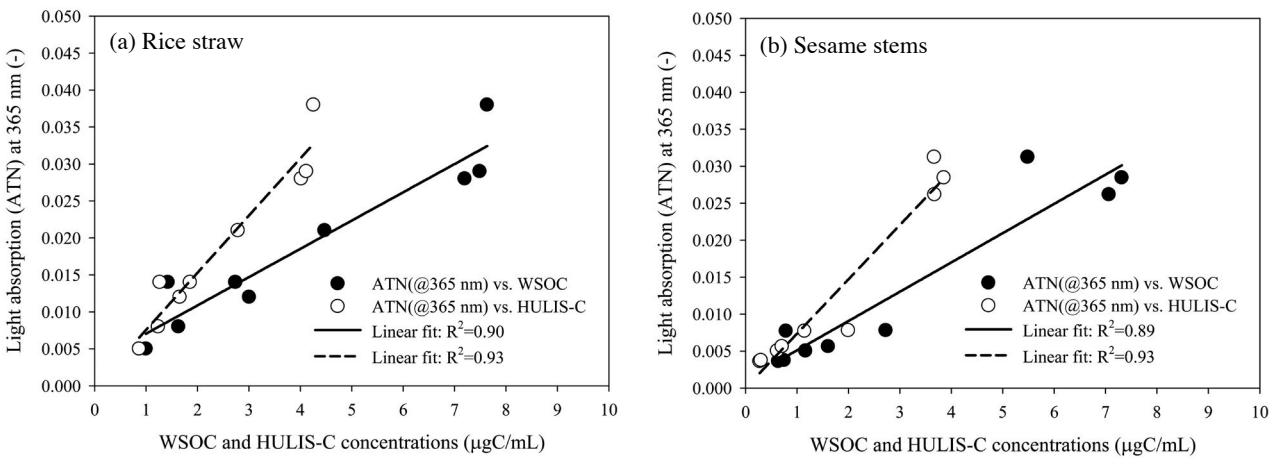

Fig. 6. Relationships of light absorption of water extracts at 365 nm with WSOC and HULIS-C concentrations for (a) rice straw and (b) sesame stems burning emissions.

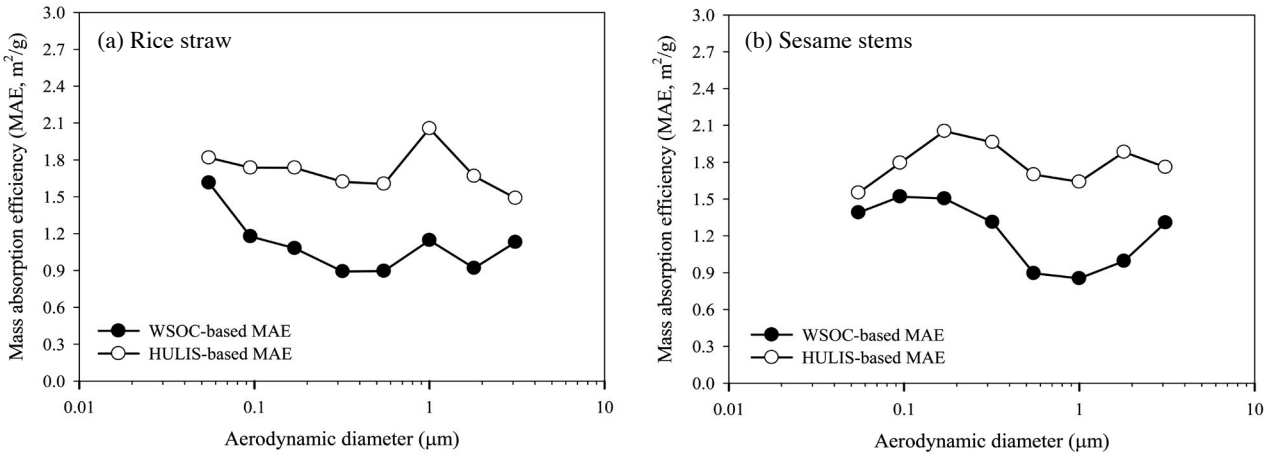

Fig. 7. Size-resolved WSOC and HULIS based mass absorption efficiencies for (a) rice straw and (b) sesame stems burning emissions

$m^2/g \cdot C$) from our previous study (Park and Yu, 2016), in which the MAE_{365} of WSOC in $PM_{2.5}$ from rice straw, pine needle, and sesame stem burning emissions was examined. Moreover, the MAE_{365} values of WSOC and HULIS-C in this study were very comparable to those of WSOM (0.79-1.56 m^2/g) and HULIS (0.97-2.09 m^2/g) from biomass smoke $PM_{2.5}$ samples (rice straw, corn straw, and pine branch), which were collected at a laboratory combustion facility (Fan *et al.*, 2016a).

4. SUMMARY AND CONCLUSION

In this study, size-segregated particulate matter (PM) smoke samples from rice straw, pine needle, and sesame stem burning emissions were collected in a laboratory combustion chamber, and analyzed to quantify the mass, OC, EC, WSOC, HULIS-C, and ionic species. Further, the light absorption properties of water extracts from size-resolved smoke samples were measured. No significant differences in size-resolved contributions of EC, WIOM, WSOM, HULIS, and SIC concentrations to PM fractions were found for each biomass type. The mean contributions of EC, WIOM, WSOM, HULIS, and SIC to the $PM_{1.8}$ were 2.6, 23.9, 50.7, 27.6 and 8.8% for the rice straw smoke samples, 7.6, 28.8, 45.2, 27.5 and 9.2% for the sesame stem smoke samples, and 12.6, 22.3, 42.2, 20.2, and 14.3% for the sesame stem smoke samples, respectively. These results were comparable to those from $PM_{2.5}$ smoke samples from the burning emissions of the three biomass materials (rice straw, pine needle, and sesame stem) (Park and Yu, 2016). EC, OC, WSOC, and HULIS-C in PM samples from the burning emissions of the three biomass materials showed unimodal size distributions that peaked at particle size range of 0.32-1.00 μm, but their modal peaks were observed to vary slightly with biomass type. This difference could be attributed to such factors as the burning conditions (temperature, smoldering or flaming, and burning rate), and amounts of biomass materials burned.

The light absorption spectra of size-resolved water extracts (WSOC) in smoke samples from BB emissions were very similar to those of brown carbon aerosol, which shows a strong tendency for the absorption to increase with decreasing wavelength in the UV and visible ranges. The light absorption spectra by WSOC showed less difference among the particle cut-sizes. The WSOC AAE values for particle cut sizes of 0.32-1.0 μm was 6.6-7.7 for rice straw smoke samples, and 7.5-8.0 for sesame stem smoke samples, respectively. Strong correlations of the light absorption of water extracts at 365 nm with WSOC and HULIS-C concentrations suggest that HULIS from BB emissions are an important contributor to the aerosol light absorption. The size-resolved MAE_{365} values of WSOC and HULIS-C based on the ratios of light absorption at 365 nm were 0.89-1.61 (average of 1.09) and 1.33-2.06 $m^2/g \cdot C$ (average of 1.82) for rice straw smoke samples, and 0.85-1.52 (average of 1.13) and 1.44-2.05 (average of 1.83) for sesame stem smoke samples, respectively. The size-resolved WSOC MAE_{365} values were comparable to those from our previous study (Park and Yu, 2016). The results of the size-resolved measurements from BB emissions could provide information to better understand the dynamic behavior of BB-affected ambient aerosols, and to evaluate the contribution of BB emissions to the light absorption by brown carbon from ambient aerosols.

ACKNOWLEDGEMENT

This research was supported by Basic Science Research Programs through the National Research Foundation of Korea (NRF) funded by the Ministry of Education (NRF-2014R1A1A4A01003896 and NRF-2017 R1D1A3A03000511). Also authors wish to acknowledge a grant-in-aid for research from Gwangju Green Environment Center (17-03-40-41-12).

REFERENCES

Altieri, K.E., Turpin, B.J., Seitzinger, S.P. (2009) Oligomers, organosulfates, and nitrooxy organosulfates in rainwater identified by ultra-high resolution electrospray ionization FTICR mass spectrometry. Atmospheric Chemistry and Physics 9, 2533-2542.

Andreae, M.O., Gelencsér, A. (2006) Black carbon or brown carbon? The nature of light-absorbing carbonaceous aerosols. Atmospheric Chemistry and Physics 6, 3131-3148.

Baduel, C., Voisin, D., Jaffrezo, J.-L. (2010) Seasonal variations of concentrations and optical properties of water soluble HULIS collected in urban environments. Atmospheric Chemistry and Physics 10, 4085-4095.

Chen, T., Bond, T.C. (2010) Light absorption by organic carbon from wood combustion. Atmospheric Chemistry and Physics 10, 1773-1787.

Cheng, Y., He, K., Du, Z., Engling, G., Liu, J., Ma, Y., Zheng, M., Weber, R.J., 2016. The characteristics of brown carbon aerosol during winter in Beijing. Atmospheric Environment 127, 355-364.

Dinar, E., Taraniuk, I., Graber, E.R., Katsman, S., Moise, T., Anttila, T., Mentel, T.F., Rudich, Y. (2006) Cloud Condensation Nuclei properties of model and atmospheric HULIS. Atmospheric Chemistry and Physics 6, 2465-2481.

Du, Z.Y., He, K.B., Cheng, Y., Duan, F.K., Ma, Y.L., Liu, J.M., Zhang, X.L., Zheng, M., Weber, R.J. (2014) A yearlong study of water-soluble organic carbon in Beijing II: light absorption properties. Atmospheric Environment 89, 235-241.

Duarte, R., Duarte, A.C. (2005) Application of non-ionic solid sorbents (XAD resins) for the isolation and fractionation of water-soluble organic compounds from atmospheric aerosols. Journal of Atmospheric Chemistry 51, 79-93.

Duarte, R., Pio, C.A., Duarte, A.C. (2005) Spectroscopic study of the water-soluble organic matter isolated from atmospheric aerosols collected under different atmospheric conditions. Analytica Chimica Acta 530, 7-14.

Fan, X., Wei, S., Zhu, M., Song, J., Peng, P. (2016a) Comprehensive characterization of humic-like substances in smoke $PM_{2.5}$ emitted from the combustion of biomass materials and fossil fuels. Atmospheric Chemistry and Physics 16, 13321-13340.

Fan, X., Song, J., Peng, P. (2016b) Temporal variations of the abundance and optical properties of water soluble Humic-Like Substances (HULIS) in $PM_{2.5}$ at Guangzhou, China. Atmospheric Research 172-173, 8-15.

Fuzzi, S., Andreae, M.O., Huebert, B.J., Kulmala, M., Bond, T.C., Boy, M., Doherty, S.J., Guenther, A., Kanakidou, M., Kawamura, K., Kerminen, V.-M., Lohmann, U., Russell, L.M., Pöschl, U. (2006) Critical assessment of the current state of scientific knowledge, terminology, and research needs concerning the role of organic aerosols in the atmosphere, climate, and global change. Atmospheric Chemistry and Physics 6, 2017-2038.

Hecobian, A., Zhang, X., Zheng, M., Frank, N., Edgerton, E.S., Weber, R.J. (2010) Water-soluble organic aerosol material and the light-absorption characteristics of aqueous extracts measured over the Southeastern United States. Atmospheric Chemistry and Physics 10, 5965-5977.

Hoffer, A., Gelencsér, A., Guyon, P., Kiss, G., Schmid, O., Frank, G.P., Artaxo, P., Andreae, M.O. (2006) Optical properties of humic-like substances (HULIS) in biomass-burning aerosols. Atmospheric Chemistry and Physics 6, 3563-3570.

Kim, H., Kim, J.Y., Jin, H.C., Lee, J.Y., Lee, S.P. (2016) Seasonal variations in the light-absorbing properties of water-soluble and insoluble organic aerosols in Seoul, Korea Atmospheric Environment 129, 234-242.

Kirillova, E.N., Andersson, A., Han, J., Lee, M., Gustafsson, Ö. (2014) Sources and light absorption of water-soluble organic carbon aerosols in the outflow from northern China. Atmospheric Chemistry and Physics 14, 1413-1422.

Kiss, G., Varga, B., Galambos, I., Ganszky, I. (2002) Characterization of water-soluble organic matter isolated from atmospheric fine aerosol. Journal of Geophysical Research 107(D21), 8339, doi:10.1029/2001 JD000603.

Krivácsy, Z., Kiss, G., Ceburnis, D., Jennings, G., Maenhaut, W., Salma, I., Shooter, D. (2008) Study of water-soluble atmospheric humic matter in urban and marine environments. Atmospheric Research 87, 1-12.

Kuang, B.Y., Lin, P., Huang, X.H.H., Yu, J.Z. (2015) Sources of humic-like substances in the Pearl River Delta, China: positive matrix factorization analysis of $PM_{2.5}$ major components and source markers. Atmospheric Chemistry and Physics 15, 1995-2008.

Laskin, A., Laskin, J., Nizkorodov, S.A. (2015) Chemistry of atmospheric brown carbon. Chemical Reviews 115, 4335-4382.

Li, C., Yan, F., Kang, S., Chen, P., Hu, Z., Gao, S., Qu, B., Sillanpää, M. (2016) Light absorption characteristics of carbonaceous aerosols in two remote stations of the southern fringe of the Tibetan Plateau, China. Atmospheric Environment 143, 79-85.

Lin, P., Huang, X.-F., He, Y.-Y., Zhen, J. (2010a) Abundance and size distribution of HULIS in ambient aerosols at a rural site in South China. Journal of Aerosol

Science 41, 74-87.
Lin, P., Engling, G., Yu, J.Z. (2010b) Humic-like substances in fresh emissions of rice straw burning and in ambient aerosols in the Pearl River Delta Region, China. Atmospheric Chemistry and Physics 10, 6487-6500.
Liu, J., Bergin, M., Guo, H., King, L., Kotra, N., Edgerton, E., Weber, R.J. (2013) Size-resolved measurements of brown carbon in water and methanol extracts and estimates of their contribution to ambient fine-particle light absorption. Atmospheric Chemistry and Physics 13, 12389-12404.
Lukács, H., Gelencsér, A., Hammer, S., Puxbaum, H., Pio, C., Legrand, M., Kasper-Giebl, A., Handler, M., Limbeck, A., Simpson, D., Preunkert, S. (2007) Seasonal trends and possible sources of brown carbon based on 2-year aerosol measurements at six sites in Europe. Journal of Geophysical Research 112, D23S18, doi:10.1029/2006JD008151.
Mayol-Bracero, O.L., Guyon, P., Graham, B., Roberts, G., Andreae, M.O., Decesari, S., Facchini, M.C., Fuzzi, S., Artaxoet, P. (2002) Water-soluble organic compounds in biomass burning aerosols over Amazonia. 2 Apportionment of the chemical composition and importance of the polyacidic fraction. Journal of Geophysical Research 107(D20), 8091, doi:10.1029/2001JD000522.
Park, S.S., Cho, S,Y., Bae, M.S. (2015) Source identification of water-soluble organic aerosols at a roadway site using a positive matrix factorization analysis. Science of the Total Environment 533, 410-421.
Park, S.S., Jeong, J.U., Cho, S.Y. (2012) Group separation of water-soluble organic carbon in ash samples from a coal combustion boiler. Asian Journal of Atmospheric Environment 6(1), 67-72.
Park, S.S., Kim, J.H. (2014) Size distribution and sources of two water-soluble organic carbon fractions at a nearby roadway site during fall season. Atmospheric Environment 94, 134-143.
Park, S.S., Schauer, J.J., Cho, S.Y. (2013a). Sources and their contribution to two water-soluble organic carbon fractions at a roadway site. Atmospheric Environment 77, 348-357.
Park, S.S., Sim, S.Y., Bae, M.S., Schauer, J.J. (2013b) Size distribution of water-soluble components in particulate matter emitted from biomass burning. Atmospheric Environment 73, 62-72.
Park, S.S., Son, S.C. (2016) Size distribution and sources of humic-like substances in an urban ambient air during winter. Environmental Science: Processes & Impacts 18, 32-41.
Park, S.S., Son, S.C. (2017) Relationship between carbonaceous components and aerosol light absorption during winter at an urban site of Gwangju, Korea. Atmospheric Research 185, 73-83.
Park, S.S., Yu, J. (2016) Chemical and light absorption properties of humic-like substances from biomass burning emissions under controlled combustion experiments. Atmospheric Environment 136, 114-122.
Rajput, P., Sarin, M.M. (2014) Polar and non-polar organic aerosols from large-scale agricultural-waste burning emissions in Northern India: Implications to organic mass-to-organic carbon ratio. Chemosphere 103, 74-79.
Saarnio, K., Aurela, M., Timonen, H., Saarikoski, S., Teinilä, K., Mäkelä, T., Sofiev, M., Koskinen, J., Aalto, P.P., Kulmala, M., Kukkonen, J., Hillamo, R. (2010) Chemical composition of fine particles in fresh smoke plumes from boreal wild-land fires in Europe. Science of the Total Environment 408, 2527-2542.
Salma, I., Meszaros, T., Maenhaut, W., Vass, E., Majer, Z. (2010) Chirality and the origin of atmospheric humic-like substances. Atmospheric Chemistry and Physics 10, 1315-1327.
Seinfeld, J.H., Pandis, S.N. (2006) Atmospheric Chemistry and Physics: From Air Pollution to Climate Change, 2nd Ed., John Wiley & Sons, Inc., New York.
Son, S.-C., Bae, M.S., Park, S.S. (2015) Chemical characteristics and formation pathways of Humic Like Substances (HULIS) in $PM_{2.5}$ in an urban area. Journal of Korean Society for Atmospheric Environment 31(3), 239-254 (in Korean with English abstract).
Turpin, B.J., Lim, H.-J. (2001) Species contributions to $PM_{2.5}$ mass concentrations: Revisiting common assumptions for estimating organic mass. Aerosol Science and Technology 35, 602-610.
Weber, R.J., Sullivan, A.P., Peltier, R.E., Russell, A., Yan, B., Zheng, M., de Gouw, J., Warneke, C., Brock, C., Holloway, J.S., Atlas, E.L., Edgerton, E. (2007) A study of secondary organic aerosol formation in the anthropogenic-influenced southeastern United States. Journal of Geophysical Research 112, D13302.
Yu, G.H., Cho, S.Y., Bae, M.S., Park, S.S. (2014) Difference in production routes of water soluble organic carbon in $PM_{2.5}$ observed during non-biomass and biomass burning periods in Gwangju, Korea. Environmental Science: Processes & Impacts 16, 1726-1736.
Zhang, X., Lin, Y.-H., Surratt, J.D., Weber, R.J. (2013) Sources, composition and absorption Angstrom exponent of light-absorbing organic components in aerosol extracts from the Los Angeles Basin. Environmental Science and Technology 47, 3685-3693.
Zheng, G.J., He, K.B., Duan, F.K., Cheng, Y., Ma, Y.L. (2013) Measurement of humic-like substances in aerosols: A review. Environmental Pollution 181, 301-314.

(Received 22 November 2016, revised 22 December 2016, accepted 22 December 2016)